

# A Four-Legs Matrix Converter Ground Power Unit with Repetitive Voltage Control

Wesam Rohouma, Pericle Zanchetta, *Member, IEEE*, Patrick W. Wheeler, *Member, IEEE*,  
Lee Empringham, *Member, IEEE*

**Abstract**—In this paper a four-legs matrix converter is proposed as the power conversion core for Aircraft Ground Power Unit (GPU) applications. This structure allows easy management of unbalanced and non-linear loads with minimal disruption of the power supply operation.

A hybrid repetitive-traditional control system is proposed to regulate the output voltage of the GPU. This solution reduces the steady state tracking error, maintaining fast dynamics characteristics, and increases the stability of the converter compared to conventional approaches.

Simulations and experimental results from a 7.5KW converter prototype are presented to verify the operation of the proposed configuration and to prove the effectiveness of the solution.

**Index Terms**— Matrix converters, Repetitive control, Cyclic Venturini modulation, Ground power unit.

## I. INTRODUCTION

There is a growing interest in using static power conversion techniques to provide very high-performance ac power supplies for use in many applications such as uninterruptible power supplies, automatic voltage regulators, programmable ac source, and ground power units (GPU) for aircraft[1].

Ground power units are designed to provide a quality three-phase supply, 400Hz to the aircraft with standard ratings up to 90 kVA per unit[2],[3],[4].

In recent years there is a rapidly growing interest in Matrix Converter technology for different applications as demonstrated by the numerous publications in the scientific literature [5-9]. The advantages of a Matrix converter (MC) over rectifier/inverter based back-to-back power converters are the controllable input power factor and the elimination of the requirement for energy storage elements in the DC link. This “all silicon” solution is particularly favourable for applications where size and weight optimization is a main concern.

Four-leg matrix converters, featuring a neutral connection as shown in, can be used to produce a balanced output voltage even under highly unbalanced or non-linear load conditions. Hence, this paper investigates its use and suitability as the power stage of a GPU for aircraft servicing.

For regulation of a converter output voltage with a 400Hz output frequency, a high bandwidth controller is required. However, the controller bandwidth is limited due to the reduced ratio between the converter control system sampling frequency and the fundamental frequency [10]. In addition, matrix converters are very prone to instability because of the presence of two resonant filters (input and output). Control design procedures and selection of the parameters need to take into account this aspect too.

To solve this problem a digital repetitive control structure including a conventional linear second order controller is proposed in this paper in a single voltage loop configuration operating in the ABC reference frame as shown in Figure 1.

Repetitive control (RC) based on the Internal Model Principle (IMP) [11-12], provides a possible control solution for systems, like this one, presenting a repetitive behaviour, to minimize or eliminate periodic waveform errors and to improve output power quality.

The use of an internal current loop is not attractive in this application due to bandwidth limitations. If an internal current loop was included, it should be much faster than the external voltage loop, which needs to be very fast itself, to be able to meet the very strict transient specifications on the output voltage required for this application. Therefore the implementation of a faster internal current loop becomes impractical with the use of standard control platforms and with the limitations on the converter switching frequency. [10, 13]. In[1] a power supply based on a four leg matrix converter has been proposed. A Genetic Algorithm (GA) procedure is used to tune the voltage control loop based on a traditional high order linear controller. However, the paper considered only a linear load case, where the supply frequency is limited to 50Hz.

This paper investigates the use of the four-leg matrix converter as a GPU application supplying linear and non linear loads at 400Hz; it presents design and practical implementation of a plug-in type repetitive control system in ABC reference in order to improve the output voltage tracking performance, during transients and in steady state, and not to affect the system stability.

## II. GPU MODULATION, DESIGN AND MODELING

Figure 1 shows the proposed topology of the 4-leg Matrix Converter based ground power unit. The circuit consists of a 3x4 array of bi-directional switches, an input filter, an output filter, and the control system. To emulate different cases of on-board loads, three load arrangements have been considered in this paper: a linear resistive inductive load, a linear resistive load and a diode bridge rectifier to emulate a non-linear load.

Manuscript received February 14, 2013; revised August 3, 2013 and October 10, 2013; accepted December 27, 2013.

Copyright © 2014 IEEE. Personal use of this material is permitted. However, permission to use this material for any other purposes must be obtained from the IEEE by sending a request to pubs-permissions@ieee.org

Wesam Rohouma is with the Department of Electrical and Electronic Engineering, University of Zawia, Lybia.

Pericle Zanchetta, Patrick W. Wheeler and Lee Empringham are with the PEMC research group, University of Nottingham, University Park, NG72RD, Nottingham, UK

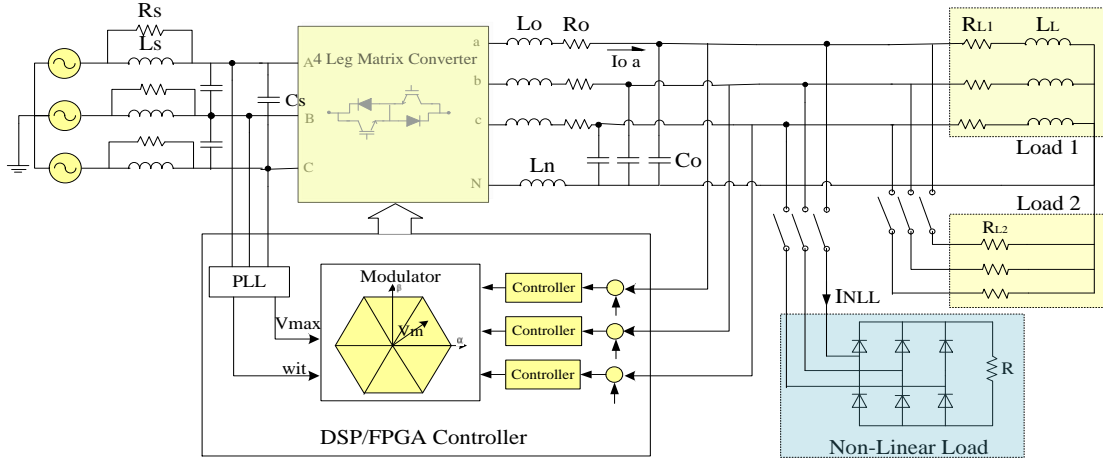


Fig. 1 Ground power unit system.

A number of different modulation methods have been proposed in literature for MCs, among which scalar methods (Venturini) and space vector methods [14-15]. The intensive research on MCs starts with the work of Venturini and Alesina in 1980 [6]. Improvements to the basic Venturini approach were made to utilize most of the volt-second area and increase the maximum output voltages from 50% of the input voltage in the basic Venturini method to 87% using the modified Venturini method.

This is possible by including the third harmonics of the input and the output quantities into the modulation process [16]. A further improvement is represented by the cyclic Venturini modulation technique, which is a modified Venturini modulation method where the switching sequence changes according to the input vector position [10, 17]. The Venturini method is preferred in this paper to a space vector approach because it deals with scalar quantities rather than vectors, and this is important when controlling unbalanced or nonlinear loads [15]. More details on the modulation used can be found in [14].

The input filter design is a result of a compromise choice between input current quality and stability of the power converter, which is substantially influenced by the input filter [18]. The values of  $L_s$ ,  $C_s$  and  $R_s$  of the chosen RLC structure are designed to keep the cut-off frequency below 2.5 kHz; this means that the input filter will be able to filter out switching harmonics in the input current while keeping the phase shift as close as possible to zero. On the other hand the LC output filter is designed to attenuate the switching ripple in the output voltage, and provide sinusoidal voltage to the load.

A good compromise solution between output power quality, filter size, weight and losses is represented by a cut-off frequency of 1100Hz, also according to the available match of capacitors and inductors. A summary of the designed parameters of the 7.5kW GPU prototype implemented in this paper are provided in Table I.

As visible in Figure 1, assuming the matrix converter has unity gain for control purposes, the open loop plant can be considered as the second order output filter plus the load.

However for control design purposes, the worst case scenario is represented by the no-load condition, since the output filter will have virtually no damping. Therefore in the following the plant is represented by only the output filter, whose transfer function can be described by (1):

$$G_p(s) = \frac{1}{s^2 + \frac{R_o}{L_o} s + \frac{1}{L_o C_o}} \quad (1)$$

With the values in Table I the plant transfer function is:

$$G_p(s) = \frac{4.901e007}{s^2 + 233.3 s + 4.901e007} \quad (2)$$

The digital control system has been implemented using a sampling rate ( $f_s$ ) of 12.8KHz. The discrete plant transfer function using zero-order-hold method is then shown in equation (3):

$$G_p(z) = \frac{0.145 z + 0.1441}{z^2 - 1.693 z + 0.9819} \quad (3)$$

TABLE I SYSTEM PARAMETERS

Supply voltage	240Vrms, 50Hz.
Input filter inductor $L_s$	600uH
Input filter capacitor $C_s$	2uF
Input filter damping resistor $R_s$	56 $\Omega$
Output filter inductor $L_o$	583uH
Output filter capacitor $C_o$	35uF
Output inductor internal resistance $R_o$	0.2 $\Omega$
Diode bridge load resistor $R$	$R=30\Omega$
Linear load 1 $R_{L1}$ and $L_L$	12 $\Omega$ , 6.25mH
Linear load 2 $R_{L2}$	19.7 $\Omega$
Sampling/Switching frequency	12800Hz
Output voltage	115Vrms, 400Hz

### III. SYSTEM CONTROL DESIGN

Control design is one of the most critical issues for this system in the view of meeting the required performance. Figure 2 shows the proposed control structure. The controller

consists of a conventional linear second order lead-lag controller  $G_c(z)$  and the plug-in repetitive controller  $G_{rc}(z)$ . The conventional controller aim is to provide the system with the required transient response characteristics and to guarantee system stability, while high precision steady state tracking can be obtained using the added repetitive controller.

#### A. Second order lead-lag controller

The second order lead-lag controller is designed using the Root Locus method with the objective of cancelling the plant poles associated with the oscillatory behavior due to the LC output filter and stabilize the system. It is used to regulate the output voltage waveform to achieve also the required transient performance.

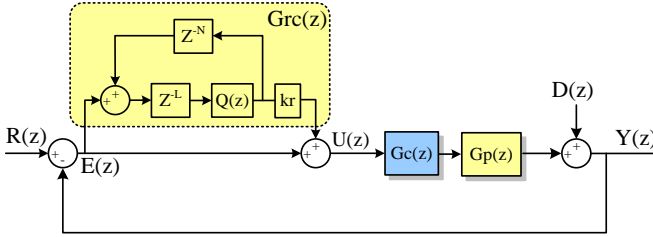


Fig. 2 Proposed control structure

Since the repetitive control will ensure steady state tracking of the 400Hz fundamental output voltage, the conventional controller poles have been chosen to be 0.99 and -0.5 to obtain a close loop bandwidth of around 200Hz. This is in order to ensure better system stability and fulfill the required transient specifications. Using direct controller design approach, the controller parameters can be found. As it can be seen in figure 2, The open loop transfer function  $G_c(z) G_p(z)$  can be described by:

$$G_p(Z)G_c(Z) = \frac{0.145 Z + 0.1441}{Z^2 - 1.693 Z + 0.9819} K_p \frac{Z^2 - 1.693Z + 0.9819}{AZ^2 + BZ + C} \quad (4)$$

Where,  $K_p$ ,  $A$ ,  $B$ ,  $C$  are the controller parameters that need to be found. The second order linear controller transfer function is given by:

$$K_p \frac{0.145 Z + 0.1441}{AZ^2 + BZ + C} \quad (5)$$

By solving the characteristics equation in the denominator of equation (5), the controller coefficients can be obtained. The solution of this equation gives a pair of poles, which can be chosen to be on the real axes inside the unit circle.

$$AZ^2 + BZ + C = (Z + Pc1)(Z + Pc2) \quad (6)$$

Using MATLAB SISOTool as shown in figure 3 the poles are found to be,  $Pc1 = -0.5$  and  $Pc2 = 0.99$ , and the controller is shown in equation (7) with  $A=1$ ,  $B=-0.495$  and  $C=0.49$ . According to Matlab SISOTool, the gain value  $K_p$  can be chosen between 0.05 and 0.4; this choice ensures that the close loop poles stay inside the unit circle. In this paper  $K_p$  is selected as 0.15, and the controller transfer function can be written as:

$$G_c(z) = 0.15 * \frac{Z^2 - 1.693Z + 0.9819}{Z^2 - 0.495Z - 0.49} \quad (7)$$

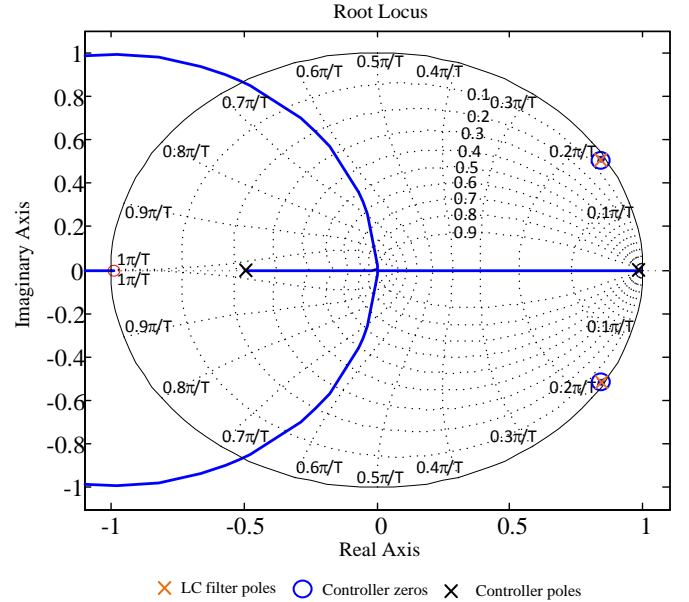


Fig. 3 Root locus of  $G_p(z)G_c(z)$

Figure 4 shows the Bode plot of the closed loop system before the insertion of the repetitive controller and it demonstrates that the system stability is achieved.

#### B. Repetitive control

As mentioned earlier the plug-in repetitive controller is added to the system to improve the steady state performance. The concept of repetitive control was originally developed in 1980 by Inoue et al. for a single input single output (SISO) plant in the continuous time domain to track a periodic repetitive signal with defined period and was then applied successfully to control a proton synchrotron magnet power supply [19]. Based on the internal model principle proposed by Francis and Wonham in 1975, any periodic reference (disturbance) signal with known period can be tracked (rejected) by including their generator in the stable closed loop [11]. Repetitive controllers have been widely used in applications including PWM inverters [20-25], PWM rectifiers [26], active power filter [27], matrix converters[10], robotic manipulators [28] and disk drive systems [29].

The plug-in RC structure used in this work is shown in Figure 2, where  $R(z)$  is the reference input,  $Y(z)$  is the output signal,  $E(z)$  is the tracking error,  $D(z)$  is a disturbance signal,  $G_c(z)$  is the second order lead-lag controller,  $G_p(z)$  is the system plant,  $G_{rc}(z)$  is the plug-in repetitive controller,  $k_r$  is the repetitive controller gain,  $Z^M$  is a delay operator,  $M$  is the number of samples in one fundamental period of the reference voltage and  $M=N+L$ ,  $Q(z)$  can be a gain lower than unity or a low pass filter to enhance the system stability and robustness.

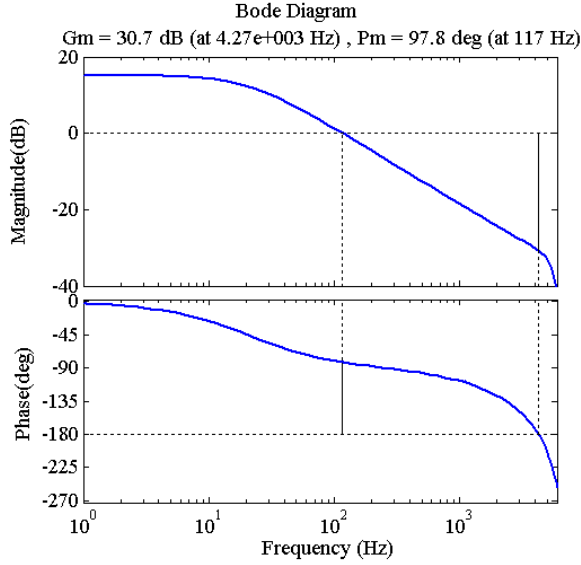


Fig. 4 Bode plot of the closed loop system without repetitive controller.

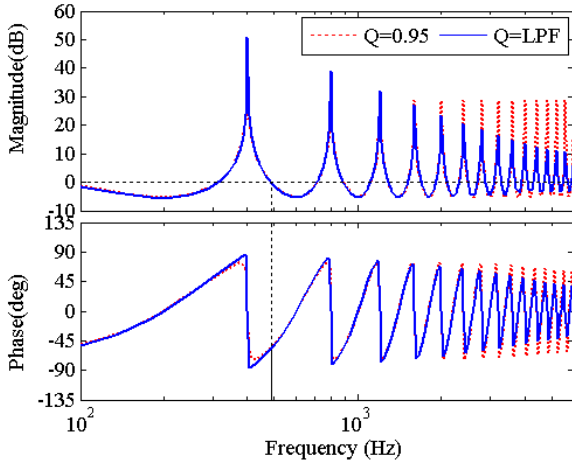


Fig. 5 Bode plot of the repetitive controller with Q as gain or LPF.

The structure and parameters values of  $Q(z)$  are designed as a trade-off between stability, robustness and error tracking. However, the choice of  $k_r$  will also affect the error convergence. A higher  $k_r$  value results in a fast error convergence but the system may become unstable [20-21].

As shown in Fig. 2 the transfer function of the repetitive controller  $G_{rc}(z)$  is given by equation (8):

$$G_{rc}(z) = \left( \frac{Z^{-L} \cdot Q(z)}{1 - Q(z) \cdot Z^{-M}} \right) \cdot K_r \quad (8)$$

The error transfer function for the whole system is:

$$\frac{E(z)}{R(z) - D(z)} = \frac{1}{1 + (1 + G_{rc}(z))G_c(z) \cdot G_p(z)} \quad (9)$$

Now by substituting equation (8) into (9) the following equation can be derived:

$$\frac{E(z)}{R(z) - D(z)} = \frac{1 - Q(z) \cdot Z^{-M}}{1 + G_c(z) \cdot G_p(z)} \cdot \frac{1}{1 - Q(z) \cdot Z^{-M} \cdot (1 - k_r \cdot H(z))} \quad (10)$$

From equation (10) it can be concluded that the whole close loop system is stable if the following two conditions are fulfilled:

1) The closed loop system without repetitive controller  $H(z)$  is stable, where the roots of  $1 + G_c(z) \cdot G_p(z) = 0$  are located inside the unit circle.

2) According to equation (10):

$$\|Q(z) \cdot (1 - k_r \cdot H(z))\| < 1, \text{ for all } z = e^{j\omega}, \omega \in [0, \pi] \quad (11)$$

According to conditions 1 and 2 the values of  $Q(z)$  and  $k_r$  can be chosen to ensure that the poles of the system are within the unit circle. Different values and structures of  $Q(z)$  (from the simple gain case to low pass FIR filter) have been tested during the design procedure, the final choice was a low pass filter  $Q(z) = 0.25Z + 0.5 + 0.25Z^{-1}$ . Increasing  $k_r$  improves the steady state error according to a given value of  $Q(z)$ . In this paper the value of  $k_r$  is selected as 0.15 to achieve a good stable system [30].

The Repetitive Controller generates a high gain at the periodic signal fundamental frequency and its integer multiples, therefore a periodic reference signal for example can be tracked provided the close loop system is stable as shown in Figure 5. The same Figure shows a comparison of the controller frequency response when using  $Q$  as a gain of 0.95 and  $Q$  as the designed low pass filter. Fig. 6 shows the bode plot of the closed loop system with and without RC, to appreciate the control effect on single harmonics.

#### IV. EXPERIMENTAL RESULTS

A prototype rated at 7.5KVA, with input line voltage of 240V, 50Hz and output phase voltage of 115V (line to neutral) at 400Hz has been successfully implemented to validate the effectiveness of the proposed GPU solution and control system. The system behaviour is tested during different conditions such as:

- Steady state condition.
- Unbalanced condition.
- Non-linear load with full wave bridge rectifier.
- Connection and disconnection of the load.

The experiments have been carried out using the system design parameters shown in table 1. The overall experimental setup of the four leg matrix converter GPU is shown in Fig. 7. 12 IGBT modules (SK60GM123) from Semikron rated at 1200V, 60A were used as bidirectional switches to implement the 3x4 matrix converter. The control system is composed of a main digital signal processor (DSP) board and an auxiliary field programmable gate array (FPGA) board. The DSP board is equipped with a TMS320C6713<sup>®</sup> device clocked at 225 MHz while the FPGA board is equipped with a ProASIC 3 A3P400<sup>®</sup> device clocked at 50 MHz.

Experimental results were captured using a LeCroy WaveSurfer 5060 oscilloscope in conjunction with an ADP300 high voltage differential voltage probe and a LeCroy CP150 current probe. Measurements were then visualized using Matlab.

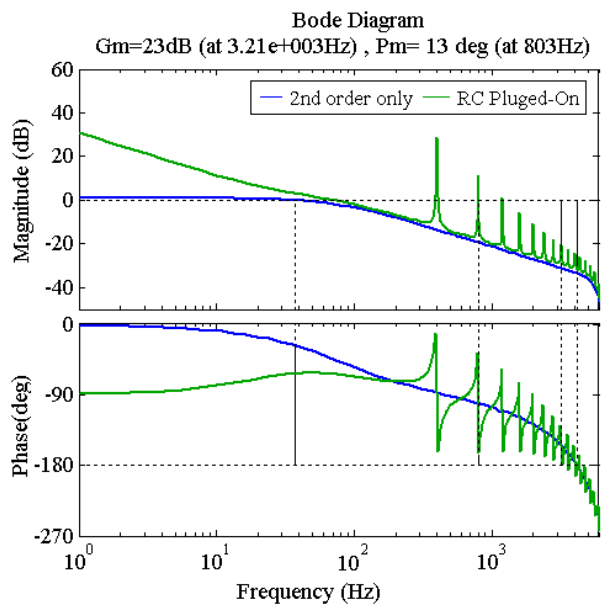


Fig. 6 Bode plot of the system with and without RC

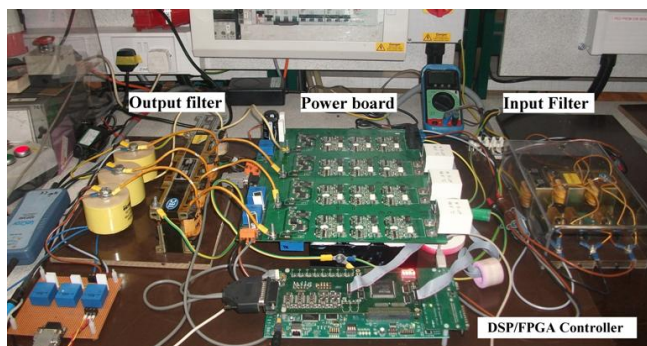


Fig. 7 Experimental setup

The following experimental results show the system response using the proposed repetitive controller in fixed ABC reference frame, during balanced, unbalanced, non-linear load and load shed scenarios. The output voltage steady state and transient's characteristics are specified in the standards BS 3G-100, BS 2G-219, ISO-6958, ISO-1540 both for military and civil aviation.

TABLE II AC NORMAL OPERATION CHARACTERISTICS  
400 HERTZ [31]

Steady state characteristics	Limits
Steady state voltage	108.0 to 118.0 V, RMS
Voltage unbalance	3.0 Volts, RMS max.
Voltage modulation	2.5 Volts, RMS maxi.
Voltage phase difference	116° to 124°
Distortion factor	0.05 maximum
Steady state frequency	393 to 407 Hz
Peak voltage	±271.8 Volts

### A. Linear load operation

The behavior of the proposed system during steady state operation is shown in Fig. 8 to Fig. 13, when feeding both linear loads 1 and 2 (Figure 1). It can be seen from Fig. 8 and Fig. 9 that the output voltage presents a very low harmonic distortion. As it can be seen in Fig. 9, the output voltage spectrum presents a harmonic peak 1% of the fundamental at 1200Hz; this peak is due to the non-linearity of the matrix converter system, namely commutation delays, and voltage drop and turn-on and turn-off of the switching devices. Fig. 10 shows that the GPU maintains the r.m.s value of the output voltage between  $\pm 3V$  of the rated 115V value as recommended in the standards BS 2G 219. Fig. 11 illustrates high accuracy voltage tracking between the output voltages and its reference using the proposed controller. The input and the output current waveforms during steady state operation are shown in Fig. 12 and Fig. 13, showing a high power quality.

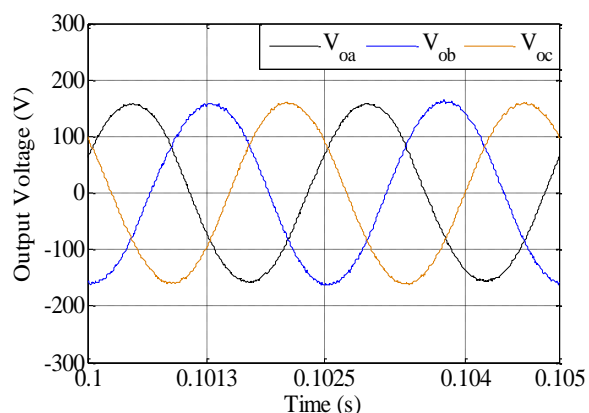


Fig. 8 Output voltages during steady state (balanced load).

### B. Unbalanced load test

Fig. 14 to Fig. 23 show the output response of the system during unbalanced loading, using load 1 (Figure 1). The percentage of unbalance implemented was more than  $\pm 50\%$ , to test the system in an extreme scenario. The load in phase A is  $5\Omega + 5.5\text{mH}$ , while in phase B  $10\Omega + 6.2\text{mH}$  and in phase C  $20\Omega + 7.5\text{mH}$  respectively. Fig. 14, Fig. 15 and Fig. 16 show that the output voltage behavior during the unbalance condition set and it can be seen that the GPU prototype is able to provide a sinusoidal output voltage with low distortion and good tracking of the reference voltage. It is important to notice that even during this extreme unbalance condition the proposed GPU was able to maintain the output voltage THD below 5%. Input and output current waveforms are shown in Fig. 17 and Fig. 18 where we can see that the output neutral current provide a path for the zero sequence components during the unbalance condition. It has to be remembered that a compromise choice needs to be made between the output voltage quality and the system stability when choosing the repetitive control gain.

### C. Non Linear Load

A three phase diode bridge rectifier circuit with a  $30\Omega$  load resistor was employed to reproduce a non-linear load effect on-board aircrafts, in parallel with load 1 (Figure 1).



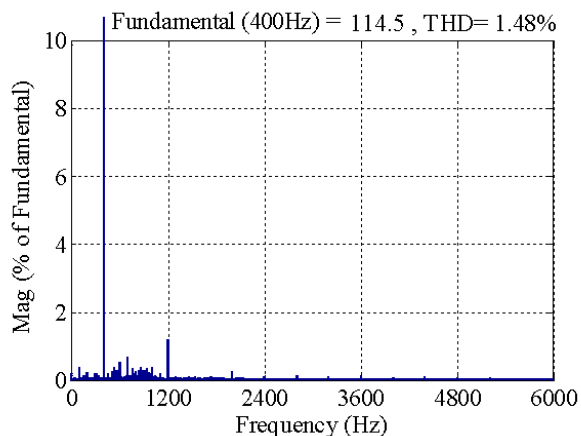


Fig. 9 FFT of output phase a voltage (balanced load).

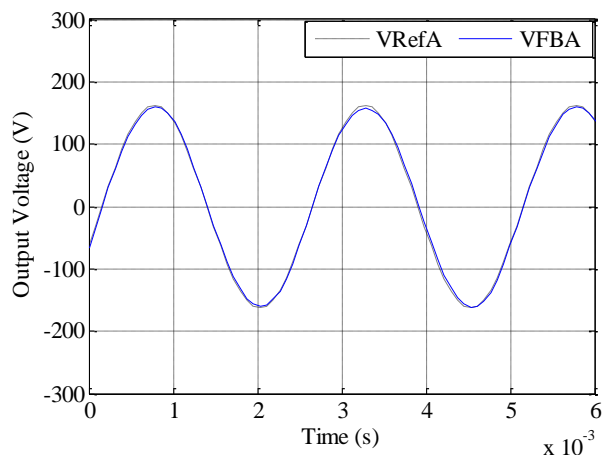


Fig. 11 Output voltage tracking (balanced load).

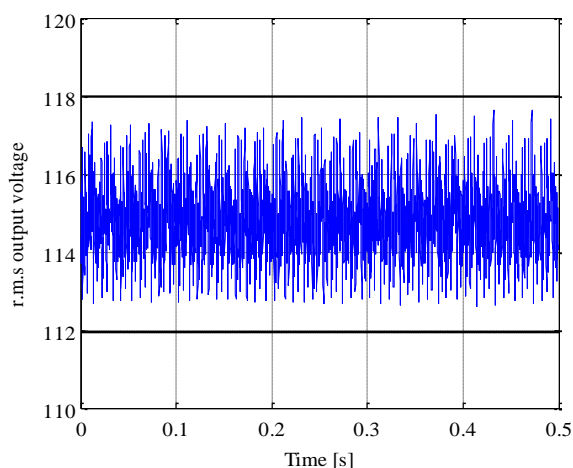


Fig. 10 R.M.S of output phase a voltage (balanced load).

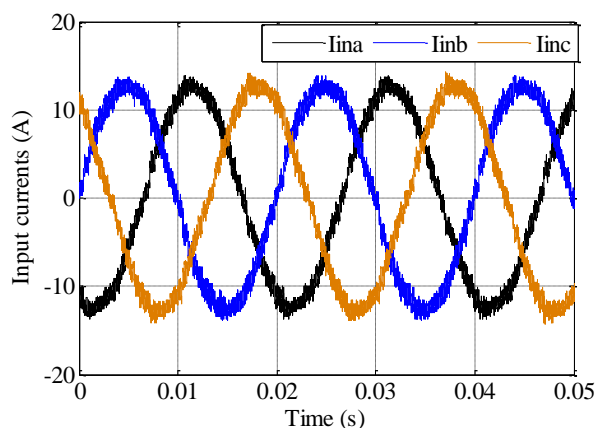


Fig. 12 Three phase input currents, balanced load

Normally 12 pulse rectifiers are used in aircraft power systems, therefore the load considered in this paper represents again a worst case scenario. Fig. 19 to Fig. 23 depict the output response to nonlinear loading. Fig. 19, Fig. 20 and Fig. 21 show that the proposed system is able to provide sinusoidal output voltages and offers a good tracking of the reference signal.

The input and output current waveforms are shown respectively in Fig. 22 (demonstrating high power quality capabilities) and Fig. 23 where the output neutral current provide a path for the zero sequence components during the unbalance conditions.

#### D. Load disconnection and connection

Fig. 24 and Fig. 25 present the performance of the proposed system in the case of sudden load disconnection and connection respectively, to test the performance of the converter during a drastic change in output current. As it can be seen, the output voltage response is very good, with only less than 23% overshoot at each transient. In this case, fast dynamic response is achieved by means of the second order lead-lag controller and high precision steady state tracking is obtained using the plug-in repetitive controller.

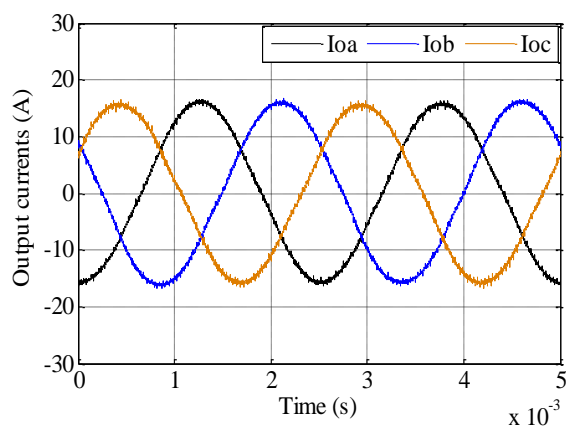


Fig. 13 Output currents (balanced load).

## V. CONCLUSIONS

This paper proposes and discusses the use of plug-in type repetitive controller to regulate the output voltage of a four-Leg matrix converter for a ground power unit application. The four-leg solution allows suitable management of unbalance load conditions with minimal supply disruption. A second order controller is used in conjunction with a plug-in repetitive controller to regulate the output voltage of the converter.

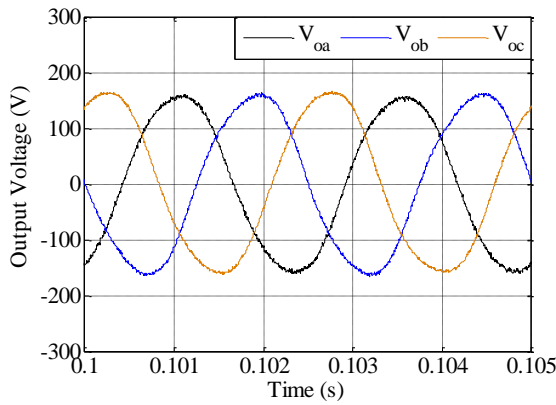


Fig. 14 Three phase output voltages (unbalanced load).

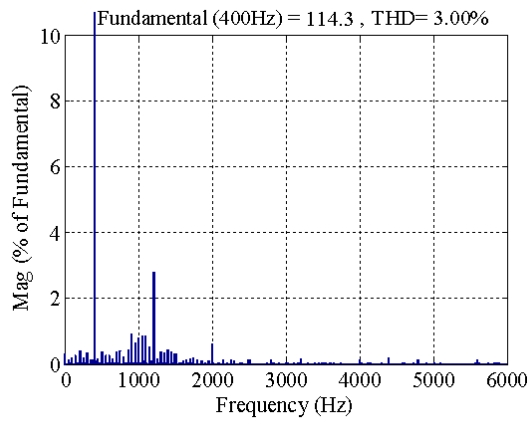


Fig. 15 FFT of output phase a voltage (unbalanced load).

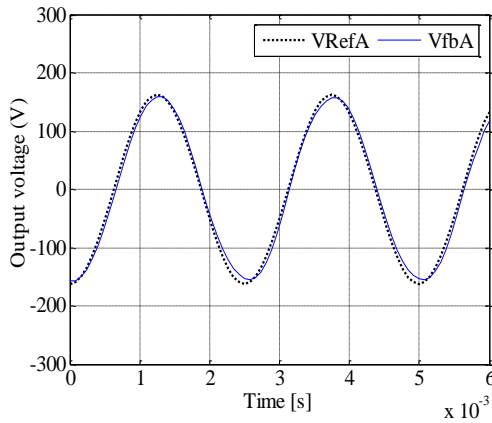


Fig. 16 Output phase a voltage tracking (unbalanced load).

The second order controller function is to improve system dynamics in transient conditions, while the repetitive controller serves to eliminate any periodic error and improve the steady state response of the system.

In addition, the presence of the repetitive controller largely improves the performance of the whole system, allowing the use of a four leg matrix converter as an AC 400Hz power supply even in the presence of non-linear loads.

This is achieved using a single voltage control loop implemented in the ABC reference frame. The use of the

proposed control structure allows the output voltage quality to comply with the strict aerospace standards. Extensive experimental tests have shown that the proposed system is able to offer high tracking accuracy, fast transient response and able to regulate the output voltage during unbalanced load conditions, nonlinear load conditions and also during load disconnection and reconnection all with minimum waveform distortion. The matrix converter solution also offers the possibility of substantial space and weight reduction.

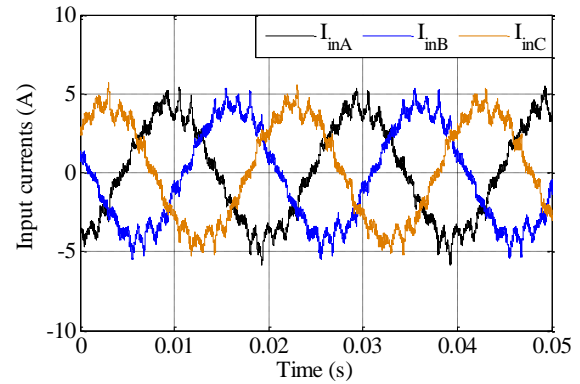


Fig. 17 Three phase input currents (unbalanced load)

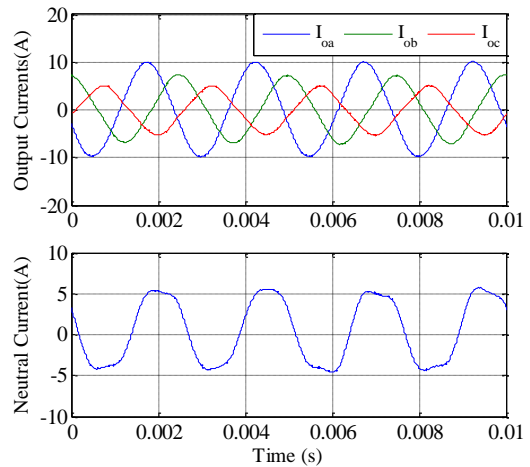


Fig. 18 Output currents and neutral current(unbalance conditions).

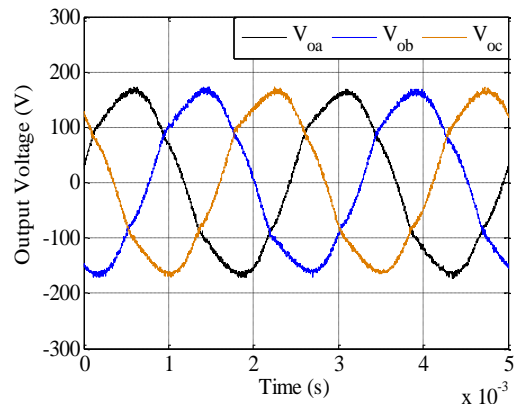


Fig. 19 Three phase output voltages (nonlinear load).

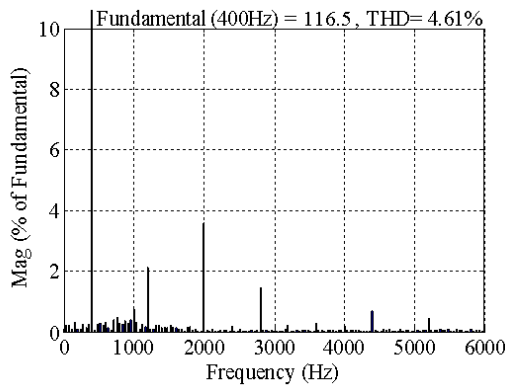


Fig. 20 Output voltage spectrum with non-linear load (phase A).

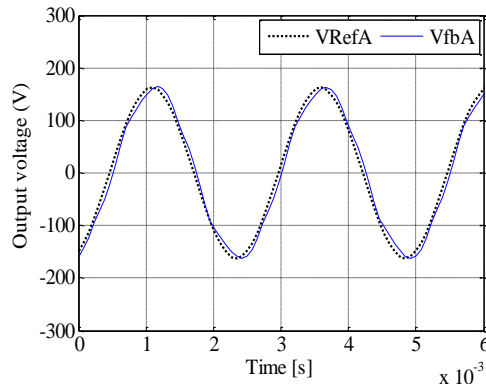


Fig. 21 Output phase a voltage tracking (Non-linear load).

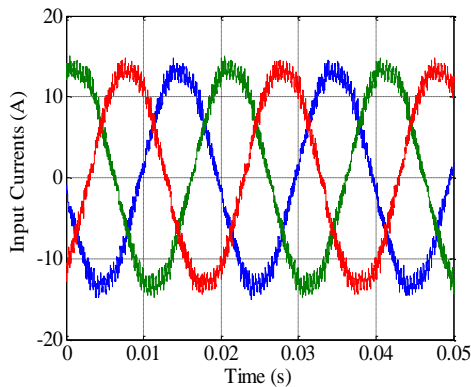


Fig. 22 Three phase input currents (non-linear load).

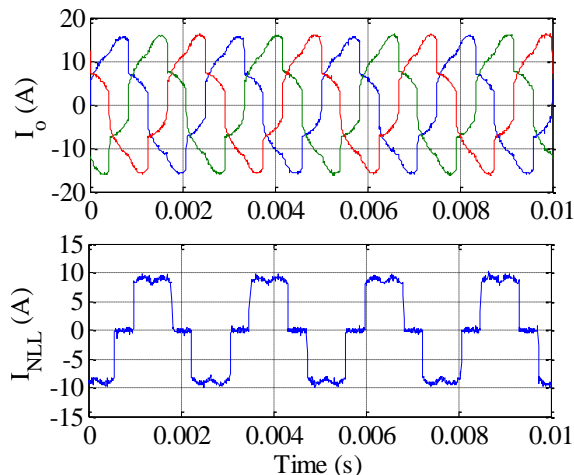


Fig. 23 Three phase output currents (non-linear load).

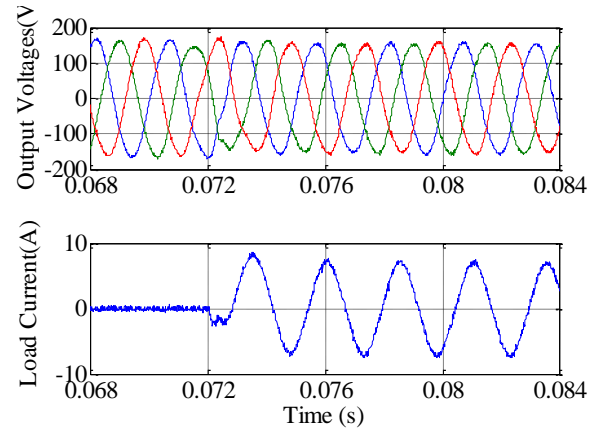


Fig. 24 Output voltage response due to load disconnection

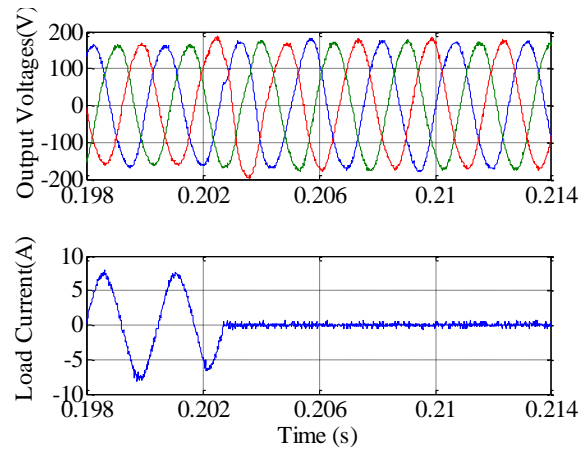


Fig. 25 Output voltage response due to load connection.

REFERENCES

- [1] P. W. Wheeler, *et al.*, "A utility power supply based on a four-output leg matrix converter," *IEEE Trans. Ind. Appl.*, vol. 44, pp. 174-186, 2008.
- [2] U. B. Jensen, *et al.*, "A new control method for 400-Hz ground power units for airplanes," *IEEE Trans. Ind. Appl.*, vol. 36, pp. 180-187, 2000.
- [3] S. Lopez Arevalo, *et al.*, "Control and implementation of a matrix converter based AC ground power supply unit for aircraft servicing," *IEEE Trans Ind. Electron.*, vol. 57, pp. 2076-2084, 2010.
- [4] S. L. Arevalo, *et al.*, "Control of a Matrix Converter-based AC Power Supply for Aircrafts under Unbalanced Conditions," *33rd Annual Conference of the IEEE Industrial Electronics Society, 2007. IECON 2007*, pp. 1823-1828.
- [5] K. Kobravi, *et al.*, "Three-Leg/Four-Leg Matrix Converter Generalized Modulation Strategy ;Part II: Implementation and Verification," *IEEE Trans Ind. Electron.*, vol. 60, pp. 860-872, 2013.
- [6] J. Rodriguez, *et al.*, "A Review of Control and Modulation Methods for Matrix Converters," *IEEE Trans Ind. Electron.*, vol. 59, pp. 58-70, 2012.
- [7] F. Villarroel, *et al.*, "Multiobjective Switching State Selector for Finite-States Model Predictive Control Based on Fuzzy Decision Making in a Matrix Converter," *IEEE Trans Ind. Electron.*, vol. 60, pp. 589-599, 2013.
- [8] J. Andreu, *et al.*, "A Step Forward Towards the Development of Reliable Matrix Converters," *IEEE Trans Ind. Electron.*, vol. 59, pp. 167-183, 2012.
- [9] L. Xiong, *et al.*, "A Three-Phase Dual-Input Matrix Converter for Grid Integration of Two AC Type Energy Resources," *IEEE*



*Trans Ind. Electron.*, vol. 60, pp. 20-30, 2013.

[10] W. M. Rohouma, *et al.*, "Repetitive control for a four leg matrix converter," *5th IET International Conference in Power Electronics, Machines and Drives (PEMD 2010)*, pp. 1-6.

[11] B. A. Francis, and Wonham, W. M., "The Internal Model Principle of Control Theory." *Automatica*. 457-465, vol. 12 (5), pp. 457-465, 1976.

[12] Y. Wang, *et al.*, "Survey on iterative learning control, repetitive control, and run-to-run control," *Journal of Process Control*, vol. 19, pp. 1589-1600, 2009.

[13] P. Zanchetta, *et al.*, "Design control and implementation of a three-phase utility power supply based on the matrix converter," *IET Power Electronics*, Vol. 2, pp. 156 - 162, 2009.

[14] P. W. Wheeler, *et al.*, "Matrix converters: a technology review," *IEEE Trans Ind. Electron.*, vol. 49, pp. 276-288, 2002.

[15] F. L. Luo, *et al.*, *Digital power electronics and applications*: Academic Press, 2005.

[16] M. P. Kazmierkowski, *et al.*, *Control in power electronics: selected problems*: Academic Pr, 2002.

[17] M. Apap, *et al.*, "Analysis and comparison of AC-AC matrix converter control strategies," *IEEE 34th Annual Power Electronics Specialist Conference, PESC 2003* pp. 1287-1292 vol.3.

[18] D. Casadei, *et al.*, "Large-Signal Model for the Stability Analysis of Matrix Converters," *IEEE Trans Ind. Electron.*, vol. 54, pp. 939-950, 2007.

[19] T. Inoue, *et al.*, "High accuracy control for magnet power supply of proton synchrotron in recurrent operation" 1980.

[20] C. Rech and J. R. Pinheiro, "New repetitive control system of PWM inverters with improved dynamic performance under non-periodic disturbances," in *IEEE Power Electronics Specialist Conference*, 2004, pp. 54-60.

[21] K. Zhang, *et al.*, "Direct repetitive control of SPWM inverter for UPS purpose," *IEEE Trans. Power Electron.*, vol. 18, pp. 784-792, 2003.

[22] C. Rech, *et al.*, "Analysis and design of a repetitive predictive-PID controller for PWM inverters," *IEEE 32nd Annual Power Electronics Specialists Conference, PESC 2001*, pp. 986-994.

[23] C. Dong, *et al.*, "An Improved Repetitive Control Scheme for Grid-Connected Inverter With Frequency-Adaptive Capability," *IEEE Trans Ind. Electron.*, vol. 60, pp. 814-823, 2013.

[24] Y. Luo, *et al.*, "High Performance Repetitive Controller for Eliminating Periodic Disturbance of Inverter with Unbalance Load," *Power and Energy Engineering Conference (APPEEC), 2012 Asia-Pacific*, 2012, pp. 1-4.

[25] M. Rashed, *et al.*, "Repetitive and Resonant Control for a Single-Phase Grid-Connected Hybrid Cascaded Multilevel Converter," *IEEE Trans. Power Electron.*, vol. 28, pp. 2224-2234, 2013.

[26] K. Zhou and D. Wang, "Digital repetitive controlled three-phase PWM rectifier," *IEEE Trans. Power Electron.*, vol. 18, pp. 309-316, 2003.

[27] Z. Zeng, *et al.*, "Research on PI and repetitive control strategy for Shunt Active Power Filter with LCL-filter," *Power Electronics and Motion Control Conference (IPEMC), 2012 7th International*, 2012, pp. 2833-2837.

[28] C. Cosner, *et al.*, "Plug in repetitive control for industrial robotic manipulators," *Robotics and Automation, 1990. Proceedings., 1990 IEEE International Conference on*, 1990, pp. 1970-1975 vol.3.

[29] J. H. Moon, *et al.*, "Repetitive control for the track-following servo system of an optical disk drive," *IEEE Trans. Control Syst. Techn.*, vol. 6, pp. 663-670, 1998.

[30] M. Jamil, *et al.*, "Current regulation of three-phase grid connected voltage source inverter using robust digital repetitive control," *International Review of Automatic Control*, vol. 4, pp. 211-219, 2011.

[31] D. o. d. i. standard, "Military standard-aircraft electric power characteristics," Department of defense interface standard. 2004.



**Wesam Rohouma** received his BSc in Electrical Engineering from the University of Zawia in 1997, his MSc in Engineering Project Managements from the University of Tripoli, Lybia in 2004 and his PhD degree in Power Electronics from the University of Nottingham, UK in 2013. From June 2013 he is Lecturer in Electrical and Electronic Engineering at the University of Zawia, Lybia, where he is also currently member of the strategic planning unit and Dean of the faculty of Engineering. His research

interests include matrix converters and control.



**Pericle Zanchetta** M(00) received his degree in Electronic Engineering and his Ph.D. in Electrical Engineering from the Technical University of Bari (Italy) in 1993 and 1997 respectively. In 1998 he became Assistant Professor of Power Electronics at the same University. In 2001 he became lecturer in control of power electronics systems in the PEMC research group at the University of Nottingham – UK, where he is now Professor in Control of Power Electronics systems. He has published over 200 peer reviewed

papers and he is Vice-Chair of the IAS Industrial Power Converter Committee IPCC. His research interests include control of power converters and drives, Matrix and multilevel converters.



**Patrick W. Wheeler** (M'00) received the Ph.D. degree in electrical engineering for his work on matrix converters from The University of Bristol, Bristol, U.K., in 1993. Since 1993, he has been with The University of Nottingham, Nottingham, U.K., where he was a Research Assistant with the Department of Electrical and Electronic Engineering and, in 1996, was a Lecturer in power-electronic systems with the Power Electronics, Machines and Control Group, where he has been a Professor since 2008. His research interests

include power-converter topologies and their applications.



**Lee Empringham** (M'10) received a B.Eng (hons) degree in Electrical and Electronic Engineering from the University of Nottingham, UK in 1996. He then joined the Power Electronics, Machines and Control Group within the School of Electrical and Electronic Engineering at the University of Nottingham, UK to work on matrix converter commutation techniques. He received his PhD degree in November 2000. Since then he has been a research fellow in the group to support different ongoing matrix converter projects. He is

currently working as a Principal Research Fellow within the group. His research interests include Direct AC-AC power conversion, Variable Speed AC Motor Drives using different circuit topologies and More-Electric Aircraft applications.